Ⅶ.　研究成果の別刷り

Magnetic Resonance Enterocolonography Is Useful for Simultaneous Evaluation of Small and Large Intestinal Lesions in Crohn's Disease

Sea Bong Hyun, MD, Yoshio Kitazume, MD, PhD,† Masakazu Nagahori, MD, PhD,* Akira Toriihara, MD,† Toshimitsu Fujii, MD, PhD,* Kiichiro Tsuchiya, MD, PhD,* Shinji Suzuki, MD, PhD,* Eriko Okada, MD, PhD,* Akihiro Araki, MD, PhD,* Makoto Naganuma, MD, PhD,* and Mamoru Watanabe, MD, PhD**

Background: We developed novel magnetic resonance enterocolonography (MREC) for simultaneously evaluating both small and large bowel lesions in patients with Crohn's disease (CD). The aim of this study was to evaluate the diagnostic performance of MREC by comparing results of this procedure to those of endoscopies for evaluating the small and large bowel lesions of patients with CD.

Methods: Thirty patients with established CD were prospectively examined by newly developed MREC. Patients underwent ileocolonoscopy (ICS) (24 procedures) or double-balloon endoscopy (DBE) (10 procedures) after MREC on the same day. Two gastroenterologists and two radiologists who were blinded to the results of another study evaluated endoscopy and MREC findings, respectively.

Results: In colonic lesions the sensitivities of the MREC for deep mucosal lesions (DML), all CD lesions, and stenosis were 88.2, 61.8, and 71.4%, respectively, while the specificities were 98.1, 95.3, and 97.7%, respectively. In small intestinal lesions, MREC sensitivities for DML, all CD lesions, and stenosis were 100, 85.7, and 100%, respectively, while specificities were 100, 90.5, and 93.1%, respectively. Endoscopic scores were significantly correlated with MREC scores. Eleven (46%) of the 24 patients who were clinically not suspected to show stricture were observed to demonstrate stricture by radiologists.

Conclusions: Our results demonstrated that MREC can simultaneously detect the CD lesions of the small and large intestine. MREC can be performed without radiation exposure, the use of enema, or the placement of a naso-jejunal catheter. MREC and endoscopy have comparable abilities for evaluating mucosal lesions of patients with CD.

(Inflamm Bowel Dis 2010;000:000–000)

Key Words: magnetic resonance enterocolonography, Crohn's disease

Crohn's disease (CD) and ulcerative colitis (UC) are chronic inflammatory bowel diseases (IBDs) associated with abdominal symptoms such as diarrhea, abdominal pain, and bloody stools. The inflammation of CD involves the entire gastrointestinal tract, particularly the small intestine. Assessing the extension and severity of the disease is critical in order to determine appropriate therapeutic strategies.[1,2] To assess whether CD lesions are present is important for patients with CD because mucosal healing has been reported to be associated with better long-term prognosis of CD.[2,3] Conventionally, evaluation of CD mainly has relied on ileocolonoscopy (ICS) and barium-based procedures, such as conventional enteroclysis (CE) and small bowel follow-through (SBFT). ICS is useful to detect inflammation in the colon and the distal end of the ileum, but the mid-small intestine is impossible to reach with this method. Because small bowel lesions are present in 4%–65% of CD patients,[4–7] conventional ICS has diagnostic limitations in detecting lesions present in CD.[4,5,7,8] SBFT is helpful for confirming the presence of fistulae or the extent of inflammation in CD. However, the detection of small erosions or aphthae by SBFT is beyond its capabilities.

Over the past few years the spectrum of diagnostic and therapeutic investigations of small bowel CD has widened considerably with recent technical advances such as wireless capsule endoscopy (WCE),[9–11] double-balloon

Additional supporting information may be found in the online version of this article.

Received for publication September 1, 2010; Accepted September 2, 2010.

From the *Department of Gastroenterology and Hepatology, †Department of Radiology, School of Medicine, Tokyo Medical and Dental University, Tokyo, Japan.

Supported in part by Health and Labour Sciences Research Grants for research on intractable diseases from Ministry of Health, Labour and Welfare of Japan.

HSB and MN (Makoto Naganuma) contributed equally to this study.

Reprints: Mamoru Watanabe, MD, PhD, Division of Gastroenterology and Hepatology, Internal Medicine, School of Medicine, Tokyo Medical and Dental University, 1-5-45 Yushima, Bunkyo-ku, Tokyo 113-8519, Japan (e-mail: mamoru.gast@tmd.ac.jp)

Copyright © 2010 Crohn's & Colitis Foundation of America, Inc.

DOI 10.1002/ibd.21510

Published online in Wiley Online Library (wileyonlinelibrary.com).

endoscopy (DBE),[12,13] high-resolution computed tomography (CT),[14] and magnetic resonance enteroclysis or enterography (MRE).[15–18] Although SBFT is widely used in CD, it carries a high radiation burden. A recent study has highlighted the high cumulative radiation dosages imparted to patients with CD.[19] In this study, CT accounted for up to 84.7% of the cumulative dose imparted to patients, and 15.5% of patients received cumulative dosage in excess of 75 mSv, which has been reported to increase cancer mortality by 7.3%. Brenner et al[20] reported that the typical mean dose imparted in adult CT use (stomach dose from abdominal scan) was 10 mSv. The carcinogenic effect of radiation can be particularly significant in patients with CD who are already at increased risk of developing gastrointestinal and hepatobiliary cancer[21] as well as small bowel lymphoma.[22]

Magnetic resonance imaging (MRI) has the potential to overcome these limitations without radiation exposure. It is characterized by a very high soft-tissue contrast, a lack of ionizing radiation, and a lower incidence of adverse events related to intravenous contrast as compared to CT.

MRE is particularly useful in providing tissue-specific information on CD at its various stages from the acute inflammatory, regenerative, fistulizing, and perforating stages to the fibrostenotic stage due to its excellent soft-tissue contrast.[15,23–27] Because conventional ICS and VCE are problematic due to CD complications, such as stenosis and fistula, the use of MRE has been expected to allow us to detect more CD lesions. However, few studies have investigated the usefulness of MRE to detect CD lesions or to distinguish CD from UC or indeterminate colitis. Furthermore, there is only one report known to us comparing the findings of magnetic resonance enterocolonography (MREC) and DBE; however, in that study the DBE procedure did not allow for the observation of ileal mucosa, in which CD lesions were frequent.[28]

The aim of this study was to evaluate the efficacy of MREC for CD lesions in the small bowel and the colon by comparing its findings to those of DBE or ICS. This is the first prospective study to evaluate both small and large bowel lesions simultaneously with the use of MREC and without enema. In the present study the severity of CD lesions on MRE were assessed and compared to endoscopic activity using a simplified endoscopic activity score for Crohn's disease (SES-CD) and a Rutgeert's score. The strictures visible on MREC were also compared to clinical symptoms or endoscopic findings.

PATIENTS AND METHODS

Patients

From July 2009 to June 2010, a total of 30 patients (20 male, 10 female; mean age 29.5 years, range 24.0–37.5) from the inpatient and outpatient departments of Tokyo Medical and Dental University Hospital were enrolled in this study. Written informed consent concerning both diagnostic procedures and participation in this prospective trial was obtained from all patients. The study was approved by the Ethics Committee of Tokyo Medical and Dental University. All patients had been diagnosed with CD using the criteria of the Research Committee on Inflammatory Bowel Disease in Japan.[29] To compare the mucosal lesions in the colon and the small intestine, DBE or ICS procedures were performed after MREC. Patients agreed to receive both MREC and DBE/ICS at entry into this study. Because hospitalization was required for DBE,[30] patients were first asked if hospitalization (3 days) was acceptable. If patients agreed to be hospitalized for DBE, they received MREC and DBE. A total of 24 patients did not consent to hospitalization; therefore, in these cases MREC and ICS were done on an outpatient basis. Thus, the small intestinal lesions proximal to the terminal ileum using MREC were compared to those obtained using 10 DBE procedures (six were done from an anal approach, four were done from an oral approach), whereas terminal ileum and colonic lesions could be assessed in all patients. Clinical disease severity was also assessed using the Crohn's Disease Activity Index (CDAI) and C-reactive protein (CRP) levels.

Reference Standards

Ten DBE and 24 ICS procedures were performed. Endoscopy was performed using video colonoscopy (ileocolonoscopy, EC-590MP, Fjinon Optical, Tokyo, Japan; double-balloon endoscopy, EN-450, Fjinon Optical). If necessary, patients were given pethidine hydrochloride (Tanabemitsubishi, Tokyo, Japan) during ICS. All patients were given midazolam (Sando, Tokyo, Japan) sedation during DBE. DBE was performed with minimum radiation for fluoroscopy.[30]

MREC

MRI was performed with a 1.5T scanner (EXCELART Vantage powered by Atlas, Toshiba Medical Systems, Japan). All MR images were acquired in a supine position with the 32 elements Atlas SPEEDER Body Coil, which covers the anterior and lateral sides of a patient's body, and the Atlas SPEEDER Spine Coil, which is embedded in the table of the MR unit. Magnesium citrate and polyethylene glycol were used for oral contrast media. Patients were given 50 g of magnesium citrate (Horii, Tokyo, Japan), which comes packaged in a powder form that the patient can reconstitute with 200 mL of water for ingestion. A typical bowel-cleansing protocol consists of ingesting the substance the day before MREC is conducted at ≈7 PM. It is then followed by ingestion of an additional

TABLE 1. Acquisition parameters of MR enterocolonography

Parameter	MR sequence			
	FASE	True SSFP	Quick 3Ds	
section orientation	coronal	coronal	axial	coronal
TR/TE (msec)	13500/78	5/2.5	5/1.9	5/1.9
flip angle (degrees)	90/140	75	13	13
fat saturation	No	No	Enhanced FatSAT	Enhanced FatSAT
SPEEDER Factor	2.0	2.0	2.2	1.8
matrix size (interpolated)	256 × 320 (320 × 320)	256 × 256 (512 × 512)	128 × 288 (528 × 576)	128 × 288 (528 × 576)
field of view (cm)	40–42	40–42	32–33 × 36–37	40–42
section thickness (interpolated) (mm)	6	4(2)	5(2.5)	5 (2.5)
section gap (mm)	0	0	0	0

Note. FASE=Fast Advanced Spin Echo, True SSFP=True Steady State Free Precession, Quick3Ds=Quick Dimensional Dynamic Diagnostic Scan, or three-dimensional gradient echo sequence, TR=repetition time, TE=echo time, FatSAT=fat saturation, SPEEDER Factor= acceleration factor of parallel imaging technique in the phase-encoding direction

200 mL of water. To further achieve an adequate distension of the distal ileum, all patients were required to drink 1000 mL-1500 mL of polyethylene glycol (PEG) (Ajinomotofarma, Tokyo, Japan) within 60 minutes before the MR, based on the patients tolerance to the PEG. Patients ingested 1000 mL of contrast medium over the initial 30 minutes, and 500 mL over the next 30 minutes. We first confirmed the liquid amount that was ingested to ensure the optimal timing of the mixture in the terminal ileum with MRI of the True SSFP (true steady state free precession). Next, FASE (fast advanced spine echo) was acquired in a coronal orientation. After 20 mg of scopolamine butylbromide (Boehringer, Tokyo, Japan) was injected intravenously to reduce bowel peristalsis, True SSFP and Quick 3Ds (quick dimensional dynamic diagnostic scan) or 3D T1-weighted gradient echo sequence were acquired in a coronal orientation. After 60 seconds of intravenous administration of gadolinium chelate (gadodiamide 0.5 mmol/L Omniscan; Daiichi Pharmaceutical, Tokyo, Japan) at a dose of 0.2 mL/kg body weight and a rate of 2 mL/s, Quick 3Ds was acquired in axial and coronal orientations. All imaging covered the entire small and large bowels and anal area. FASE, True SSFP, and Quick 3Ds in the axial orientation were acquired during a single breath-hold. However, Quick 3Ds in the axial required individuals to hold their breath twice. Acquisition parameters are listed in Table 1.

Segmentation for MREC and Endoscopy of CD

The small bowel was divided into three distinct anatomic sections for the purposes of analysis.[11] In MREC analyses, these sections were determined relative to the position of the small bowel in the abdominal cavity: the jejunum section, located in the left upper quadrant (LUQ) of the abdomen; the ileum segment, located in the left lower quadrant (LLQ), the segment corresponding to bowel loops located in the right upper and lower quadrant (RULQ); and the terminal ileum segment extending 10 cm from the ileocecal valve. The colon and terminal ileum were divided into five distinct anatomic sections based on SES-CD.[31] The lesions in the terminal ileum, right colon segment, transverse colon, left colon segment, and rectum segment were separately scored and evaluated. To assess the severity of CD lesions in each segment, the most severe lesion in each segment was selected to be scored by MREC, ICS, and DBE.

Classification and Evaluation of CD Lesions for MREC and Endoscopies

Endoscopic and MREC findings in each segment for the individual patient were classified as in Table 2. The morphologic severities in CD lesions were classified in the following manner: no pathologic changes (NPC: 0), superficial mucosal lesions (SML: 1), and deep mucosal lesions (DML: 2). In the present study, scars were defined as NPC. In the endoscopic findings, edema, erythema, and aphthoid lesions were classified as SML, whereas ulcers, fissures, and lesions with a cobblestone appearance were classified as DML (Table 2).[11] The presence of at least two indicative criteria for each category was needed to diagnose as SML or DML. The per-segment comparisons between MREC and endoscopies only included those segments that were evaluated by both modalities.

Next, endoscopic severity of CD lesions in the colon and terminal ileum was scored by SES-CD for each

TABLE 2. Criteria at endoscopy and MREC for classification of small and large bowel lesion of CD

	endoscopic findings	imaging findings at MREC
A. morphologic changes	0) NPC: no pathologic changes (no mucosal or mural pathology)	
	1) SML: superficial mucosal lesion	
		• subtly increased contrast enhancement
	• edema	• subtle irregularity of the fold pattern
	• erythema	• no wall thickening
	• aphtous without ulcerous lesions	• no submucosal edema
		• no extra-mural hypervascularity
	2) DML: deep mucosal lesion	
		• markedly increased contrast uptake
		•wall thickening>4mm
	• ulcers	• disrupted the fold pattern
	• fissures	• cobble stone
	• cobble stone pattern	• deep mucosal fissures
		• submucosal edema
		• extra-mural hypervascularity
	absent = no obstruction	
	present = obstruction	
B. obstruction		
	incomplete through the stenotic lesion	luminal narrowing(<11 mm) and consensus of radiologist about presence of radiologic stenoses

patient.[31] To be compared with SES-CD, MRCE score was also defined in this study by modifying SES-CD as shown in Table 3.

For the evaluation of endoscopic findings, exclusively in the small intestine, each segment severity was also scored using a modified Rutgeert's score[32]: grade 0a indicates the absence of small bowel lesions; grade 0b indicates stricture without inflammation; grade 1 indicates five or fewer aphthoid lesions; grade 2 indicates more than five aphthoid lesions; grade 3 indicates diffuse aphthous ileitis with diffusely inflamed mucosa; grade 4 indicates diffuse inflammation with larger ulcers; and grade 5 indicates ulcerated stricture. Grades 0a and 0b were considered inactive disease, whereas grades 1+ reflected active disease. For the comparison, severity of each small intestine segment was assessed in MREC as well, as shown in Table 2.

Stricture was also assessed in accordance with "B. Obstruction" in Table 2. The severity of stricture was scored (1 = very unlikely, 2 = unlikely, 3 = not sure, 4 = likely, 5 = very likely) both by clinicians in charge of each patient and radiologists who interpreted the MREC.[33] Correlation coefficients and kappa scores were then calculated to determine the agreement between clinical and radiologic assessments of stricture.

Image Interpretation

Two independent physicians performed endoscopies, and two board-certified radiologists assessed the MRCE findings. Both the physicians and radiologists were blinded to the patient clinical presentation and the results of the other studies (endoscopic or MRI findings) as well.

TABLE 3. Criteria at MREC score based on SES-CD

Variable	0	1	2	3
size of ulcers, wall thickness, highly enhancement, and deep depressions	none	aphthousulcers (ϕ 0.1 to 0.5 cm)	largeulcers (ϕ 0.5 to 2 cm)	very large ulcers (ϕ > 2cm)
ulcerated surface	none	<10%	10–30%	>30%
affected surface when present hyperintensity on T2 relative to the signal of psoas muscle, and slightly enhancement on T1	none	<50%	50–75%	>75%
presence of narrowing	>11mm	11–6mm	6mm>	6–0mm

TABLE 4. Clinical characteristics of 30 patients at inclusion into the study

female, n (%)	10 (33)
mean age at examination (IQR)	29.5 (24.0–37.5)
mean disease duration (month) (IQR)	48.5 (14.3–150.3)
mean BMI (IQR)	198 (181–217)
disease location	
ileal, n (%)	8 (26)
ileocolonic, n (%)	20 (67)
colonic, n (%)	2 (7)
perianal involvement,n (%)	4 (13)
symptomatic, n (%)	20 (67)
mean CDAI score (IQR)	82 (42–138)
CDAI>150, n (%)	7 (23)
mean CRP(mg/dL) (IQR)	0.31 (0.05–0.83)
CRP>0.3mg/dL	16 (53)
previous surgery, n (%)	11 (37)
concomitant treatments	
5-ASA, n (%)	11 (37)
steroids, n (%)	3 (10)
immunosuppressants, n (%)	10 (33)
anti-TNF antibodies, n (%)	6 (20)
no medication, n (%)	7 (23)

Statistical Methods

All statistical analyses were performed with standard statistical software. JMP8 (SAS Institute, Cary, NC) was used for statistical analysis. Spearman correlation coefficients (two-sided) were determined to examine associations between endoscopic score, MRI score, CDAI, CRP, and stricture likelihood scores. Kappa scores were also calculated to examine the agreement between clinicians and radiologists on the likelihood of stricture. *P*-values less than 0.05 were considered significant.

RESULTS

MREC Is Comparable to Conventional ICS in the Detection of CD Lesions in the Terminal Ileum and Colon of CD Patients

The patients clinical characteristics are shown in Table 4. MREC and ICS/DBE were performed on the same day in all patients. Ten patients did not have abdominal symptoms and MREC/endoscopies were performed for screening. Another 20 patients received MREC/endoscopies to assess the severities and extension of disease due to abdominal symptoms (Table 4). Supporting Table 1 details the endoscopic and MREC findings in the small and large intestines of all patients. DML was observed in 35 (23%) of the 150 segments by MREC, while in 34 (24%) of the 140 segments by ICS/DBE. SML could be detected in the terminal ileum and colonic segments less frequently in MRCE (3 [2%] of 150 segments) than in endoscopy (20 [14%] of 140 segments). Eighteen patients (60%) exhibited either SML or DML in the terminal ileum or colon by MREC. Stenosis was observed in nine patients (30%) by MREC. MREC sensitivities for DML, any CD lesion (both SML and DML), and stenosis were 88.2, 61.8, and 71.4%, respectively, while specificities were 98.1, 95.3, and 97.7%, respectively (Fig. 1a). An example of the classification and scoring is shown

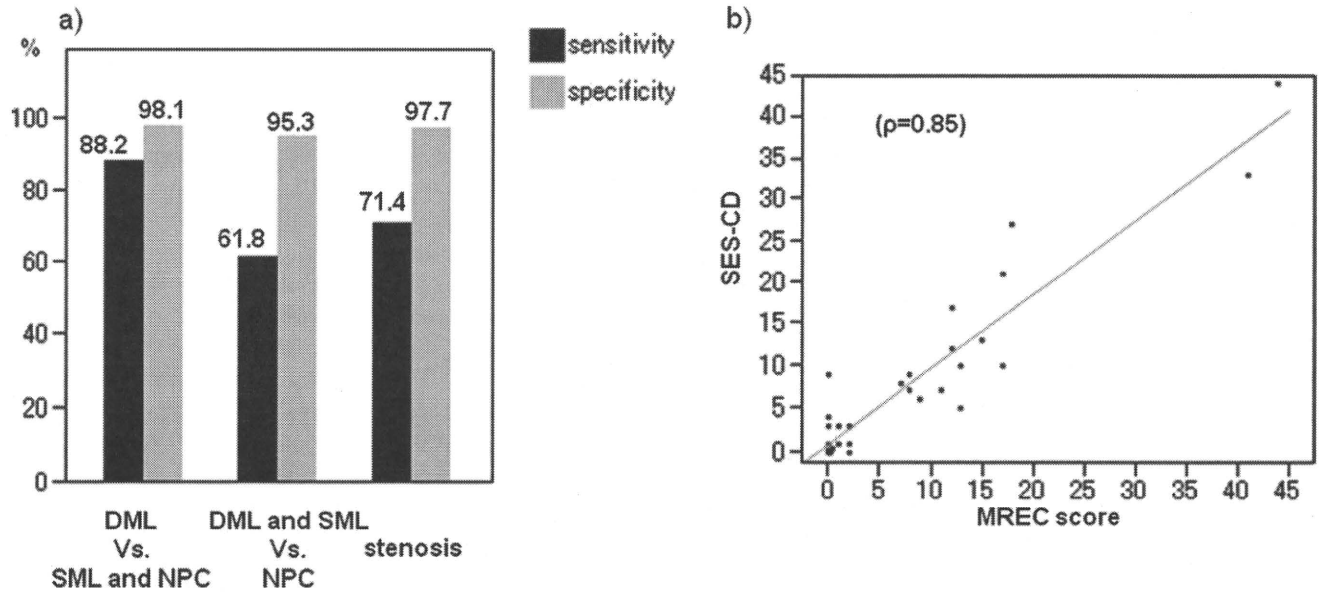

FIGURE 1. Diagnostic capabilities of MRCE in the assessment of terminal ileum and colonic lesions. (a) The sensitivity and specificity of MREC for DML, any CD lesions (DML + SML), and stenosis. (b) Correlation between MREC scores and SES-CD scores.

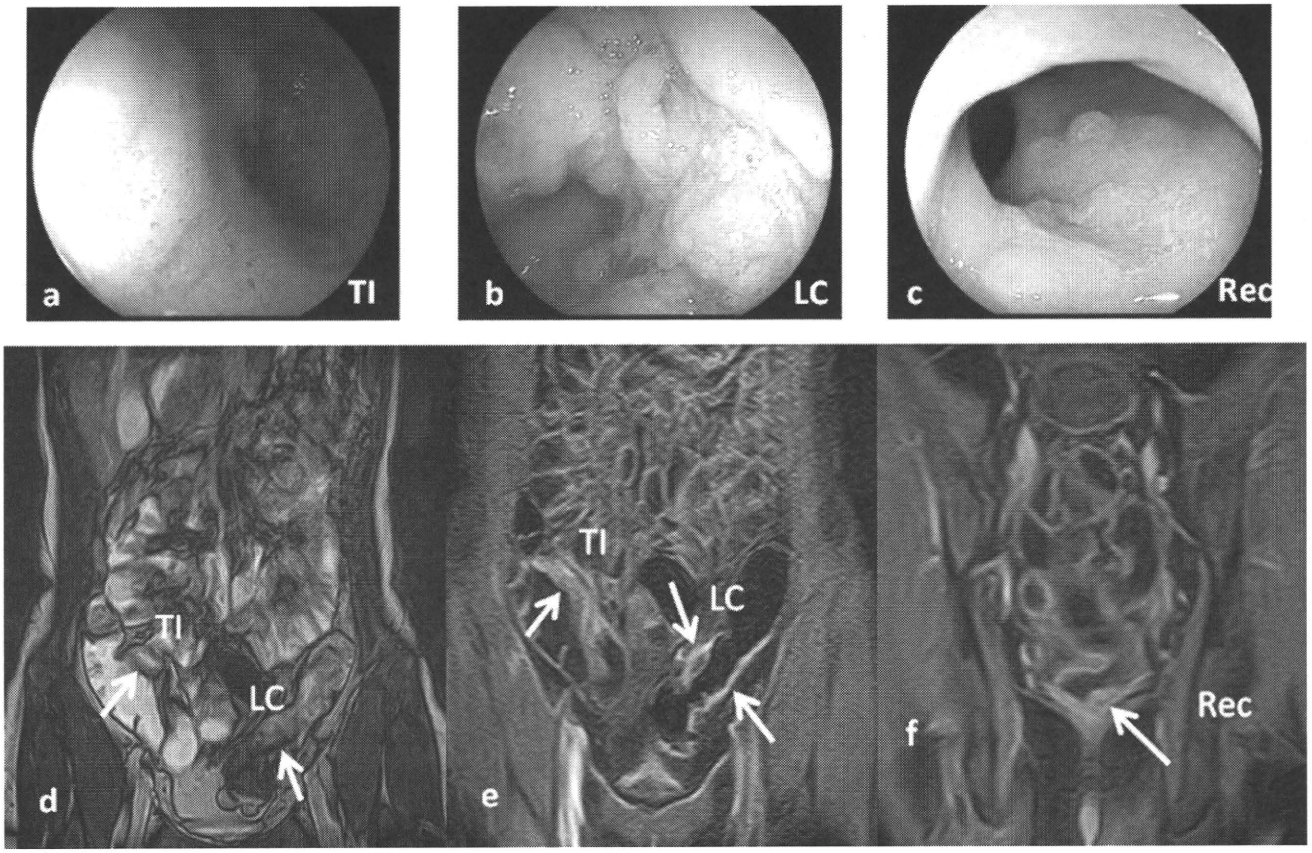

FIGURE 2. An example of comparison between endoscopy and MREC in terminal ileum and colonic lesions. Conventional colonoscopy detected DMLs in the terminal ileum (a), sigmoid colon (b), and rectum (c). MREC with True SSFP sequence in coronal view (d) and 3D T1-weighted contrast-enhanced GRE sequence (e,f; coronal view) in a patient with multifocal CD. TI: terminal ileum, LC: left sided colon, Rec: rectum.

in Figure 2. Wall thickening, mucosal irregularities, markedly increased contrast enhancement by MREC were indicative of DML. Figure 1b indicates that a strong correlation ($\rho = 0.85$, $P < 0.0001$) was found between SES-CD (median 5.5, interquartile range [IQR] 1.0–10.5) and MREC score (median 4.5, IQR 0–13.3) in terminal ileum and colonic lesions. Both CDAI and CRP moderately correlated with endoscopic and MREC scores (CDAI versus SES-CD; $\rho = 0.56$, $P = 0.001$, CDAI versus MREC score; $\rho = 0.41$, $P = 0.024$, CRP:SES-CD; $\rho = 0.40$, $P = 0.025$, CRP versus MREC score; $\rho = 0.36$, $P = 0.049$). These results indicate that MREC was comparable to colonoscopy in the detection of terminal ileum and colonic lesions.

MREC Is Useful in the Detection of CD Lesions in the Small Intestine

Because the usefulness of MREC for the detection of CD lesions in the small intestine has not been well investigated, we assessed the detection rate of CD lesions in the jejunum, ileum, and terminal ileum by MREC. Twenty-seven DML lesions (30%) and 3 (3%) SML lesions were observed in 90 segments by MRE. Surprisingly, any small intestine lesions were found in 23 (77%) of 30 patients.

Next we compared CD lesions detected by MREC with those obtained by DBE. Most intestinal lesions observed by MREC were consistent with those by DBE. For the small intestinal lesions, the sensitivities of MREC in detecting DML, any CD lesions (12 DML and 2 SML), and stenosis were 100 (12/12), 85.7 (12/14), and 100% (6/6), respectively, while the specificities were 100 (25/25), 90.5 (19/21), and 93.1% (130/133), respectively (Fig. 3a). Figure 4 indicates an example where stenosis could be detected by MREC, which could not be reached by DBE because of another distal stricture.

There was also a strong correlation ($\rho = 0.88$, $P < 0.0001$) between Rutgeert's scores (median 0, IQR 0–4) and MREC scores (median 0, IQR 0–2) for small bowel lesions (Fig. 3b). CDAI moderately correlated with Rutgeert's scores ($\rho = 0.44$, $P = 0.03$), and weakly correlated with MREC scores ($\rho = 0.25$, $P = 0.24$). CRP did not

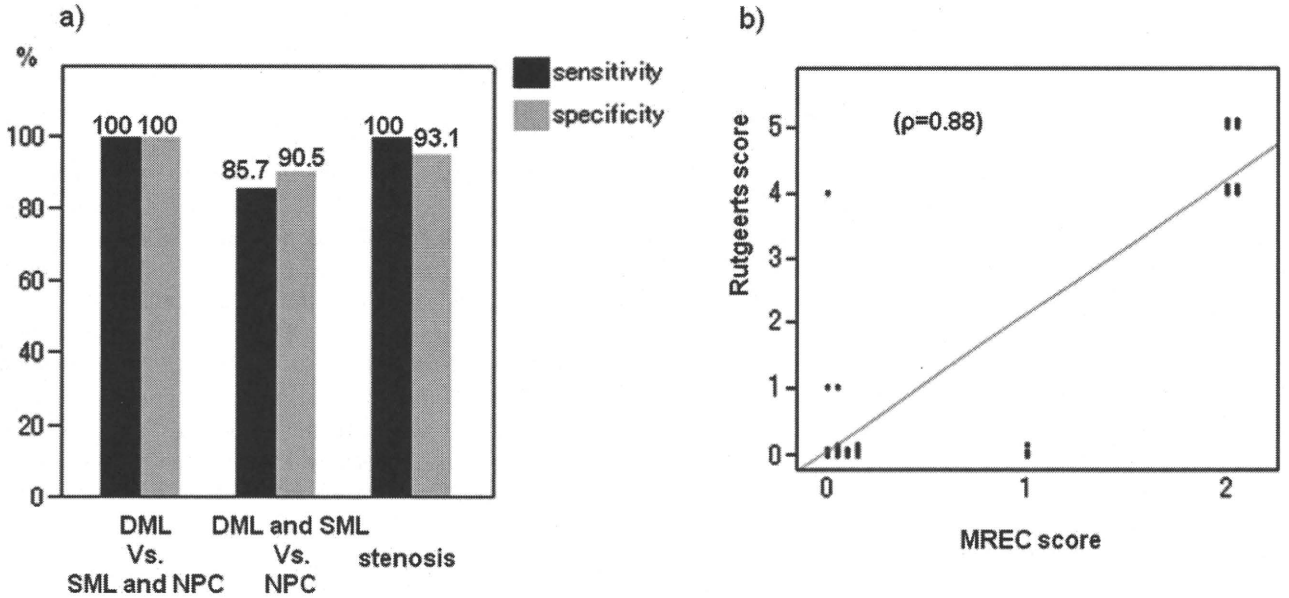

FIGURE 3. Diagnostic capabilities of MRCE in the assessment of the small intestinal lesions. (a) The sensitivity and specificity of MREC for DML, any CD lesions (DML + SML), and stenosis. (b) Correlation between MREC scores and Rutgeert's scores for CD lesions in the small intestine.

correlate with Rutgeert's scores ($\rho = 0.11$, $P = 0.61$) or MREC scores ($\rho = 0.10$, $P = 0.65$). These results suggest that MREC is comparable to DBE in detecting active lesions in the small intestine.

Physicians' Assessment for Strictures May Be Consistent with Findings from MREC

A moderate correlation ($\rho = 0.57$, $P = 0.001$) and kappa score (0.32, $P < 0.001$) were calculated, demonstrating

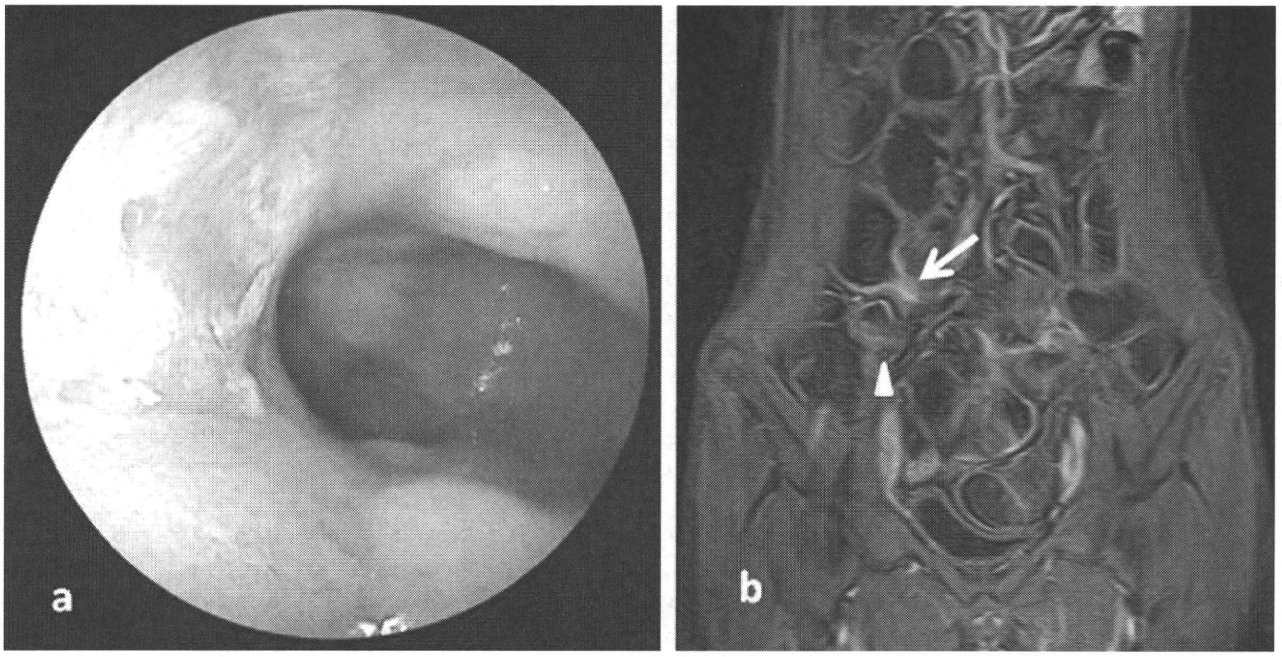

FIGURE 4. An example of cases where ileal stenosis was detected by DBE (a) and MREC (b). (a) DBE revealed severe stenosis with deep longitudinal ulceration in the terminal segment of the ileum. DBE instrument could not be passed through the stenosis. (b) MREC detected the ileal lesion (white arrow). Furthermore, multifocal DML (arrowhead) above the distal stenosis was also detected.

TABLE 5. Agreement between clinical and radiologic stenosis

clinical likelihood of stenosis	radiologic stenosis	
	present	absent
very unlikely or unlikely	11	13
not sure, likely, or very likely	6	0

Kappa = 0.32 (95% CI: 0.12–0.58).

the fair level of agreement between clinical and radiologic assessments. Interestingly, radiologists pointed out stenosis in 11 (46%) patients who did not have obstructive symptoms (Table 5).

DISCUSSION

Previously, Rimola et al[34] demonstrated that MRE is useful for detecting disease activity and assessing severity of CD lesions in the colon and terminal ileum. However, they did not evaluate CD lesions in the jejunum and proximal to terminal ileum. Furthermore, rectal balloon catheter was retrogradely instilled when MRE was done. Seiderer et al[28] also showed the usefulness of MR enteroclysis to evaluate the CD lesions in the small intestine; however, a nasojejunal catheter was used in that study. Our study is the first prospective report to evaluate jejunal, ileal, and colonic CD lesions simultaneously using MREC. It should be emphasized that gastroduodenal intubation and enema were not needed to perform MREC in the present study. We also confirmed that MREC demonstrated high sensitivity and specificity for CD lesions such as DML and stenosis. MREC was able to detect lesions in the small intestines of 23 (77%) of 30 patients. Our study also indicated that the sensitivity of MREC for stenosis in the large bowel was 71.4% and that in the small bowel was 100%. Interestingly, jejunal and ileal CD lesions (inflammation, stenosis) beyond the first stenosis were detectable with MREC, although endoscopies could not pass through the first one. Furthermore, the severity detected with MREC was closely correlated with that obtained with endoscopies. These results suggest that MREC can be a useful tool in the detection of CD lesions without excessive pain/radiological exposure.

Our study also indicated that MREC was less sensitive than endoscopy for the detection of superficial lesions. Another study showed that MRE was inferior to VCE for the detection of mucosal lesions consistent with CD. However, the long-term prognosis of CD patients with superficial small-bowel lesions is unknown. Thus, MREC is thought to be a useful modality despite its potential for misdiagnosis of the small lesions of CD patients.

DBE is the only method that allows for tissue sampling and pathological examination in the jejunum and ileum. Histological examination can provide valuable information to aid in assessing the severity of inflammatory changes. Therefore, DBE can be used to diagnose CD in inconclusive cases in which histological diagnosis would alter treatment strategy.[35] However, the disadvantages of DBE for CD patients should be emphasized as well. First, adhesions and fistulas are frequently observed in CD patients and can result in technical difficulties of observing the entire small intestine. Second, it is impossible to observe the mucosa along the entire length of the small intestine using either the oral or anal approach in one session of DBE. It was difficult to observe the entire small intestine in some cases, even though both oral and anal approaches to DBE were conducted. Finally, DBE is accompanied by severe complications in $\approx$1% of cases. With the use of MREC, observation of both the entire small intestine and colon were possible and were less complicated than with DBE.

Most patients would likely prefer MRE to MR enteroclysis because of reduced abdominal discomfort and nausea.[36,37] When MR enteroclysis is performed, patients are still exposed to radiation during the placement of the nasojejunal catheter. Moreover, the complicated logistics of using two diagnostic rooms in tandem needs to be considered. A prospective randomized study showed similar diagnostic sensitivities for MRE and MR enteroclysis (88 versus 88%).[36] Therefore, we performed MRE to detect CD lesions.

In the present study, patients ingested a total of 1500 mL contrast medium, as previously described,[38] with 1000 mL ingested over the initial 30 minutes and 500 mL ingested 30 minutes later. It should be emphasized that patients were administrated magnesium citrate oral contrast media 1 day prior to the administration of MREC in this study. This method could potentially enable radiologists to evaluate colonic lesions more easily.

Our prospective evaluation indicated that clinical and radiologic assessments of stricture were significantly correlated. This correlation was greater in the colonic lesion and in small intestinal lesion. A kappa score (kappa = 0.32) was also calculated and confirmed the significant agreement. Our results are consistent with the results (kappa = 0.34) of Higgins et al,[33] which showed that assessment using CT enterography was comparable to clinical assessment for strictures. Radiological findings were significantly correlated, but discrepancies between radiological and clinical assessments were observed in 11 patients. This result suggests that MREC has the possibility to detect the obstructive lesions before patients have abdominal symptoms.

There are some limitations to our study. Our patient group was very small and was possibly preselected

considering the relatively high prevalence of multifocal small bowel disease, which may not be representative of a general CD population. Despite the small number of patients, we believe that our study has value as a preliminary or exploratory study. Future studies should include the enrollment of a larger number of patients to obtain more conclusive results.

In conclusion, MREC demonstrated comparative ability to endoscopy for the simultaneous assessment of both small and large intestinal lesions in a follow-up of CD patients. Additionally, the technique was accompanied by minimal risks and no radiation exposure. Moreover, our results suggest that MREC can enable clinicians to detect strictures or severe lesions early in the course of the disease. Because of the minimal risk involved in MREC, this diagnostic tool can be repeated. Recently, mucosal healing has been reported to be critical for the long-term prognosis of CD. MREC may be useful in confirming improvement of the CD lesions in both large and small bowel as a result of intensive treatments, such as infliximab.

ACKNOWLEDGMENT

The authors thank American Journal Experts for article revision in English.

REFERENCES

1. Mary JY, Modigliani R. Development and validation of an endoscopic index of the severity for Crohn's disease: a prospective multicentre study. Groupe d'Etudes Therapeutiques des Affections Inflammatoires du Tube Digestif (GETAID). *Gut.* 1989;30:983–989.
2. Schnitzler F, Fidder H, Ferrante M, et al. Mucosal healing predicts long-term outcome of maintenance therapy with infliximab in Crohn's disease. *Inflamm Bowel Dis.* 2009;15:1295–1301.
3. Frøslie KF, Jahnsen J, Moum BA, et al. Mucosal healing in inflammatory bowel disease: results from a Norwegian population-based cohort. *Gastroenterology.* 2007;133:412–422.
4. Wagtmans MJ, van Hogezand RA, Griffioen G, et al. Crohn's disease of the upper gastrointestinal tract. *Neth J Med.* 1997;50:S2–7.
5. van Hogezand RA, Witte AM, Veenendaal RA, et al. Proximal Crohn's disease: review of the clinicopathologic features and therapy. *Inflamm Bowel Dis.* 2001;7:328–337.
6. Ochsenkuhn T, Herrmann K, Schoenberg SO, et al. Crohn disease of the small bowel proximal to the terminal ileum: detection by MR-enteroclysis. *Scand J Gastroenterol.* 2004;39:953–960.
7. Lescut D, Vanco D, Bonniere P, et al. Perioperative endoscopy of the whole small bowel in Crohn's disease. *Gut.* 1993;34:647–649.
8. Otterson MF, Lundeen SJ, Spinelli KS, et al. Radiographic underestimation of small bowel stricturing Crohn's disease: a comparison with surgical findings. *Surgery.* 2004;136:854–860.
9. Dubcenco E, Jeejeebhoy KN, Petroniene R, et al. Capsule endoscopy findings in patients with established and suspected small-bowel Crohn's disease: correlation with radiologic, endoscopic, and histologic findings. *Gastrointest Endosc.* 2005;62:538–544.
10. Papadakis KA, Lo SK, Fireman Z, et al. Wireless capsule endoscopy in the evaluation of patients with suspected or known Crohn's disease. *Endoscopy.* 2005;37:1018–1022.
11. Tillack C, Seiderer J, Brand S, et al. Correlation of magnetic resonance enteroclysis (MRE) and wireless capsule endoscopy (CE) in the diagnosis of small bowel lesions in Crohn's disease. *Inflamm Bowel Dis.* 2008;14:1219–1228.
12. Yamamoto H, Sekine Y, Sato Y, et al. Total enteroscopy with a nonsurgical steerable double-balloon method. *Gastrointest Endosc.* 2001; 53:216–220.
13. May A, Nachbar L, Ell C. Double-balloon enteroscopy (push-and-pull enteroscopy) of the small bowel: feasibility and diagnostic and therapeutic yield in patients with suspected small bowel disease. *Gastrointest Endosc.* 2005;62:62–70.
14. Sailer J, Peloschek P, Schober E, et al. Diagnostic value of CT enteroclysis compared with conventional enteroclysis in patients with Crohn's disease. *AJR Am J Roentgenol.* 2005;185:1575–1581.
15. Gourtsoyiannis NC, Papanikolaou N, Karantanas A. Magnetic resonance imaging evaluation of small intestinal Crohn's disease. *Best Pract Res.* 2006;20:137–156.
16. Prassopoulos P, Papanikolaou N, Grammatikakis J, et al. MR enteroclysis imaging of Crohn disease. *Radiographics.* 2001;21:S161–172.
17. Herrmann KA, Michaely HJ, Seiderer J, et al. The "star-sign" in magnetic resonance enteroclysis: a characteristic finding of internal fistulae in Crohn's disease. *Scand J Gastroenterol.* 2006;41:239–241.
18. Herrmann KA, Michaely HJ, Zech CJ, et al. Internal fistulas in Crohn disease: magnetic resonance enteroclysis. *Abdom Imaging.* 2006;31: 675–687.
19. Desmond AN, O'Regan K, Curran C, et al. Crohn's disease: factors associated with exposure to high levels of diagnostic radiation. *Gut.* 2008;57:1524–1529.
20. Brenner D, Elliston C, Hall E, et al. Estimated risks of radiation-induced fatal cancer from pediatric CT. *AJR Am J Roentgenol.* 2001; 176:289–296.
21. Bernstein CN, Blanchard JF, Kliewer E, et al. Cancer risk in patients with inflammatory bowel disease: a population-based study. *Cancer.* 2001;91:854–862.
22. Jess T, Loftus EV Jr, Velayos FS, et al. Risk of intestinal cancer in inflammatory bowel disease: a population-based study from Olmsted County, Minnesota. *Gastroenterology.* 2006;130:1039–1046.
23. Frokjaer JB, Larsen E, Steffensen E, et al. Magnetic resonance imaging of the small bowel in Crohn's disease. *Scand J Gastroenterol.* 2005;40:832–842.
24. Herrmann KA, Zech CJ, Michaely HJ, et al. Comprehensive magnetic resonance imaging of the small and large bowel using intraluminal dual contrast technique with iron oxide solution and water in magnetic resonance enteroclysis. *Invest Radiol.* 2005;40:621–629.
25. Low RN, Sebrechts CP, Politoske DA, et al. Crohn disease with endoscopic correlation: single-shot fast spin-echo and gadolinium-enhanced fat-suppressed spoiled gradient-echo MR imaging. *Radiology.* 2002; 222:652–660.
26. Maccioni F, Bruni A, Viscido A, et al. MR imaging in patients with Crohn disease: value of T2- versus T1-weighted gadolinium-enhanced MR sequences with use of an oral superparamagnetic contrast agent. *Radiology.* 2006;238:517–530.
27. Maccioni F, Viscido A, Broglia L, et al. Evaluation of Crohn disease activity with magnetic resonance imaging. *Abdom Imaging.* 2000;25: 219–228.
28. Seiderer J, Herrmann K, Diepolder H, et al. Double-balloon enteroscopy versus magnetic resonance enteroclysis in diagnosing suspected small-bowel Crohn's disease: results of a pilot study. *Scand J Gastroenterol.* 2007;42:1376–1385.
29. Yao T, Matsui T, Hiwatashi N. Crohn's disease in Japan: diagnostic criteria and epidemiology. *Dis Colon Rectum.* 2000;43:S85–93.
30. Araki A, Tsuchiya K, Okada E, et al. Single-operator double-balloon endoscopy (DBE) is as effective as dual-operator DBE. *J Gastroenterol Hepatol.* 2009;24:770–775.
31. Daperno M, D'Haens G, Van Assche G, et al. Development and validation of a new, simplified endoscopic activity score for Crohn's disease: the SES-CD. *Gastrointest Endosc.* 2004;60:505–512.
32. Colombel JF, Solem CA, Sandborn WJ, et al. Quantitative measurement and visual assessment of ileal Crohn's disease activity by computed tomography enterography: correlation with endoscopic severity and C reactive protein. *Gut.* 2006;55:1561–1567.
33. Higgins PD, Caoili E, Zimmermann M, et al. Computed tomographic enterography adds information to clinical management in small bowel Crohn's disease. *Inflamm Bowel Dis.* 2007;13:262–268.

34. Rimola J, Rodriguez S, Garcia-Bosch O, et al. Magnetic resonance for assessment of disease activity and severity in ileocolonic Crohn's disease. *Gut*. 2009;58:1113–1120.
35. Bourreille A, Ignjatovic A, Aabakken L, et al. Role of small-bowel endoscopy in the management of patients with inflammatory bowel disease: an international OMED-ECCO consensus. *Endoscopy*. 2009; 41:618–637.
36. Negaard A, Paulsen V, Sandvik L, et al. A prospective randomized comparison between two MRI studies of the small bowel in Crohn's disease, the oral contrast method and MR enteroclysis. *Eur Radiol*. 2007;17:2294–2301.
37. Negaard A, Sandvik L, Berstad AE, et al. MRI of the small bowel with oral contrast or nasojejunal intubation in Crohn's disease: randomized comparison of patient acceptance. *Scand J Gastroenterol*. 2008;43:44–51.
38. Lee SS, Kim AY, Yang SK, et al. Crohn disease of the small bowel: comparison of CT enterography, MR enterography, and small-bowel follow-through as diagnostic techniques. *Radiology*. 2009;251:751–761.

Suppression of *Hath1* Gene Expression Directly Regulated by Hes1 Via Notch Signaling Is Associated with Goblet Cell Depletion in Ulcerative Colitis

Xiu Zheng, MD, Kiichiro Tsuchiya, MD, PhD, Ryuichi Okamoto, MD, PhD, Michiko Iwasaki, MD, PhD, Yoshihito Kano, MD, Naoya Sakamoto, MD, PhD, Tetsuya Nakamura, MD, PhD, and Mamoru Watanabe, MD, PhD

Background: The transcription factor *Atoh1/Hath1* plays crucial roles in the differentiation program of human intestinal epithelium cells (IECs). Although previous studies have indicated that the Notch signal suppresses the differentiation program of IEC, the mechanism by which it does so remains unknown. This study shows that the undifferentiated state is maintained by the suppression of the *Hath1* gene in human intestine.

Methods: To assess the effect of Notch signaling, doxycycline-induced expression of Notch intracellular domain (NICD) and Hes1 cells were generated in LS174T. *Hath1* gene expression was analyzed by quantitative reverse-transcription polymerase chain reaction (RT-PCR). Hath1 promoter region targeted by HES1 was determined by both reporter analysis and ChIP assay. Expression of Hath1 protein in ulcerative colitis (UC) was examined by immunohistochemistry.

Results: Hath1 mRNA expression was increased by Notch signal inhibition. However, Hath1 expression was suppressed by ectopic HES1 expression alone even under Notch signal inhibition. Suppression of the *Hath1* gene by Hes1, which binds to the 5′ promoter region of Hath1, resulted in suppression of the phenotypic gene expression for goblet cells. In UC, the cooperation of aberrant expression of HES1 and the disappearance of caudal type homeobox 2 (CDX2) caused Hath1 suppression, resulting in goblet cell depletion.

Conclusions: The present study suggests that Hes1 is essential for *Hath1* gene suppression via Notch signaling. Moreover, the suppression of Hath1 is associated with goblet cell depletion in UC. Understanding the regulation of goblet cell depletion may lead to the development of new therapy for UC.

(Inflamm Bowel Dis 2011;000:000–000)

Key Words: ulcerative colitis, Hath1, Hes1, Notch signaling

The gut epithelium undergoes continual renewal throughout adult life, maintaining the proper architecture and function of the intestinal crypts. This process involves highly coordinated regulation of the induction of cellular differentiation and the cessation of proliferation, and vice versa.[1–3] Many studies of the regulation of intestinal differentiation have shown that cellular formation of the villi in small and large intestine is affected by various intracellular signaling pathways such as Notch, Wnt, and BMP.[4–7] Moreover, recent studies have also shown that dysregulation of the differentiation system for prompt intestinal epithelial cell formation induces the pathology of such intestinal diseases as colon cancer, Crohn's disease and ulcerative colitis (UC).[8] Then it was suggested that crucial genes for the differentiation of intestinal epithelium cells (IECs) become corrupt by aberrant cell signaling on the pathogenesis of intestinal diseases.

One of the most important genes for cell formation is a basic helix-loop-helix (bHLH) transcription factor, *Atoh1*, and its human homolog, *Hath1*, which is essential for the differentiation toward secretory lineages in small and large intestine.[9] Using a ubiquitin proteasomal system, we demonstrated that regulation of Hath1 protein in colon carcinogenesis is regulated by glycogen synthase kinase 3β (GSK3β) via Wnt signaling. Moreover, Hath1 and β-catenin protein are reciprocally regulated by GSK3β in Wnt signaling for the coordination between cell differentiation and

Additional Supporting Information may be found in the online version of this article.

Received for publication November 9, 2010; Accepted November 15, 2010.

From the Department of Gastroenterology and Hepatology, Graduate School, Tokyo Medical and Dental University, Tokyo, Japan.

Supported in part by grants-in-aid for Scientific Research 19209027, 21590803, 21790651, and 21790653, from the Japanese Ministry of Education, Culture, Sports, Science and Technology; JFE (Japanese Foundation for Research and Promotion of Endoscopy); Japan Foundation for Applied Enzymology; Intractable Diseases, the Health and Labor Sciences Research Grants from the Japanese Ministry of Health, Labor and Welfare.

The first two authors contributed equally to this work.

Reprints: Mamoru Watanabe, MD, PhD, MD, PhD, Professor and Chairman, Department of Gastroenterology and Hepatology, Graduate School, Tokyo Medical and Dental University, 1-5-45 Yushima, Bunkyo-ku, Tokyo 113-8519, Japan (e-mail: mamoru.gast@tmd.ac.jp)

Copyright © 2011 Crohn's & Colitis Foundation of America, Inc.

DOI 10.1002/ibd.21611

Published online 00 Month 2011 in Wiley Online Library (wileyonlinelibrary.com).

proliferation. These findings together indicate that the deletion of adenomatous polyposis coli (APC) in colon carcinogenesis causes Hath1 protein degradation by switching the target of GSK3β from β-catenin to Hath1, resulting in maintenance of the undifferentiated state.[10] The dysregulation of prompt differentiation of IEC thus causes major intestinal diseases, and elucidation of the roles of various cell-signaling pathways in intestine is therefore important in understanding the pathogenesis of intestinal diseases.

We have also recently reported aberrant expression of Notch intracellular domain (NICD) in lesions showing goblet cell depletion in UC patients.[8] Moreover, forced expression of NICD caused the suppression of phenotypic genes for goblet cells in human intestinal epithelial cells. It has also been reported that forced expression of NICD in murine intestinal epithelial cells caused the depletion of goblet cells with the decrease of Atoh1 expression.[5] Thus, it is likely that *Atoh1* gene expression is regulated by Notch signaling, leading to subsequent control of intestinal epithelial cell lineage decision of the crypt cells.

The regulation of Hath1, however, is less well understood in human intestine. In previous reports, regulation of *Atoh1* gene expression was assessed using the mouse or chicken promoter region,[11,12] but the critical domains of the mouse and chicken sequences are not completely conserved in the Hath1 promoter region and enhancer region. To date, the regulation of *Hath1* gene expression has not been assessed using the human sequence. In particular, it remains unknown how *Hath1* gene expression is suppressed by Notch signaling in the intestine. It also remains unknown whether goblet cell depletion in UC is affected by Hath1 expression in intestinal epithelial cells.

In this study we demonstrated that Hes1 expression via Notch signaling is enough to suppress the *Hath1* gene by directly binding to the 5′ promoter region of Hath1. In UC, the cooperation of Hes1 and caudal type homeobox 2 (CDX2) caused the suppression of Hath1, resulting in the goblet cell depletion.

MATERIALS AND METHODS

Cell Culture

Human colon carcinoma-derived LS174T cells were maintained in minimum essential medium supplemented with 10% fetal bovine serum and 1% penicillin-streptomycin, 4 mM L-glutamine. Except where indicated otherwise, cells were seeded at a density of 5×10^5 cells/mL in each experiment. Cell cultures and transfections of plasmid DNA were performed as previously described.[6] A cell line expressing Notch1 intracellular domain (NICD), Hes1, HeyL (Tet-On NICD, Tet-On Hes1, Tet-On HeyL cells) under the control of doxycycline (DOX, 100 ng/mL, ClonTech, Palo Alto, CA) was generated as previously described.[8] The cell lines were supplemented with Blastcidin (7.5 μg/mL, Invitrogen, La Jolla, CA) and Zeocin (750 μg/mL, Invitrogen) for maintenance. The inhibition of Notch signaling was achieved by the addition of LY411,575 (1 μM).

Quantitative Real-time Polymerase Chain Reaction (PCR)

Total RNA was isolated with Trizol reagent (Invitrogen) according to the manufacturer's instructions. Aliquots of 1 μg of total RNA were used for cDNA synthesis in 20 μL of reaction volume. One microliter of cDNA was amplified with Cyber Green in a 20-μL reaction as previously described.[6] The primer sequences in this study are summarized in Supporting Information Table S1.

Plasmids

5′ Hath1 reporter plasmid was generated by cloning a 1031-bp sequence 5′ of the human *Hath1* gene (corresponding to −1,029 to +2 of the promoter region) into a pGL4 basic vector (Promega, Madison, WI). Hath1 reporter plasmid containing the 3′ region was generated by cloning a 4811-bp sequence 3′ of the human *Hath1* gene (corresponding to +1401 to +6211 of the Hath1 genome) into the 5′ Hath1 reporter plasmid. Internal deletion mutants of the 5′ Hath1 reporter plasmid in which three Hes1 binding sites CACGCG (−305 to −300, −269 to −264, −159 to −154) were replaced with GTCGAC were constructed by PCR-mediated mutagenesis.[13] Doxycycline-dependent expression of NICD was achieved by cloning the gene encoding the intracellular portion of the mouse Notch1 into the pcDNA4/TO/myc-his vector (Invitrogen).[8] Doxycycline-dependent expression of Hes1 was achieved by cloning the gene encoding rat Hes1 into the pcDNA4/TO/myc-his vector (Invitrogen). Doxycycline-dependent expression of HeyL was achieved by cloning the gene encoding human HeyL into the pcDNA4/TO/myc-his vector (Invitrogen). All constructs were confirmed by DNA sequencing.

Luciferase Assays

LS174T cell seeded in a 6-well plate culture dish were transfected with 4 μg of reporter plasmid along with 10 ng of pRL-tk plasmid (Promega). Cells were harvested 36 hours after transfection, lysed by three cycles of freezing and thawing, and the luciferase activities in each sample as indicated by arbitrary unit were normalized against Renilla luciferase activities as previously described.[10]

Chromatin Immunoprecipitation Assay

A chromatin immunoprecipitation (ChIP) assay was performed essentially as previously described with some modifications.[6] LS174T/Hes1 cells were seeded onto a 150-mm dish, then stimulated with DOX or left untreated for 12 hours. Immunoprecipitation was performed overnight at 4°C with 10 μg of an anti-Hes1 (a kind gift from Dr. T. Sudo), normal mouse immunoglobulin G (sc-2025, Santa Cruz Biotechnology, Santa Cruz, CA), or an anti-histone H3 antibody (Abcam,

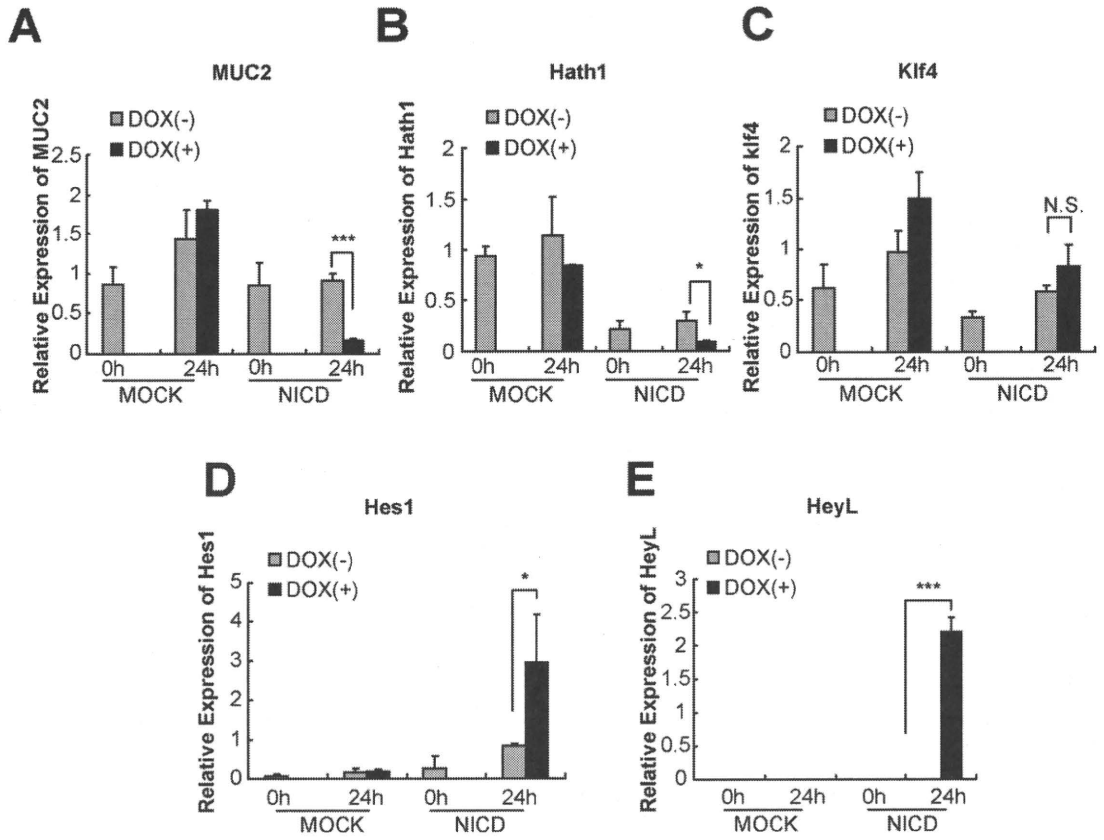

FIGURE 1. Gene alternation in LS174T cells by the expression of NICD. NICD is induced by DOX using the Tet-on system to mimic the acceleration of the Notch signal in LS174T cells. NICD expression by DOX decreased the expression of MUC2 (A) and Hath1 (B) genes. Klf4 gene expression was not affected (C). NICD also induced expression of Hes family genes such as Hes1 (D) and HeyL (E). (*$P < 0.05$, ***$P < 0.001$, $n = 3$).

Cambridge, MA). The genomic DNA fragments in the immunoprecipitated samples were analyzed by PCR using primers indicating the positions on the genomic DNA relative to the translation start site (Supporting Information Table 1). The same amounts of DNA samples were analyzed by conventional PCR in parallel with the following parameters: denaturation at 94°C for 15 seconds, annealing at 60°C for 30 seconds, and extension at 68°C for 60 seconds for 45 cycles. The products were resolved by agarose gel electrophoresis, stained with ethidium bromide, and visualized using an ImageQuant TL system (GE Healthcare, Milwaukee, WI).[6] The primer sequences in this study are summarized in Supporting Information Table S1.

Human Intestinal Tissue Specimens

Human tissue specimens were obtained from patients who underwent endoscopic examination or surgery at Yokohama Municipal General Hospital or Tokyo Medical and Dental University Hospital. Normal colonic mucosa was obtained from patients with colorectal cancer who underwent colectomy. Each of three patients with UC and colon cancer were examined. Written informed consent was obtained from each patient and the study was approved by the Ethics Committee of both Yokohama Municipal General Hospital and Tokyo Medical and Dental University.

Immunohistochemistry

Hath1 antibody (1:5000) was originally generated as previously described. Hes1 antibody (1:10,000) was the same as in the ChIP assay. Fresh frozen tissue was used after microwave treatment (500W, 10 minutes) in 10 mM citrate buffer for Hath1 and Hes1. The standard ABC method (Vectastain; Vector Laboratories, Burlingame, CA) was used, and staining was developed by addition of diaminobenzidine (Vector Laboratories).

Statistical Analyses

Quantitative real-time PCR analyses were statistically analyzed with Student's *t*-test. *P* less than 0.05 was considered statistically significant.

RESULTS

Notch Signaling Suppresses *Hath1* Gene Expression But Not Kuppel-like Factor 4 (Klf4) Gene in Human IECs

Expression of Atoh1 seems to be regulated at its transcriptional level, as forced expression of NICD in murine IECs causes the decrease of Atoh1 mRNA expression and subsequent depletion of goblet cells in vivo.[5] We therefore assessed the effect of the Notch signal on the expression of

Hath1 in a human intestinal epithelial cell line, LS174T cells. NICD is induced by DOX using a Tet-on system to mimic the acceleration of the Notch signal. NICD expression showed not only the decrease of Mucin2 (MUC2) expression but also a significant decrease of *Hath1* gene expression (Fig. 1A,B). We also assessed Klf4 gene expression by NICD expression because Klf4 is also essential to goblet cell differentiation.[14] Klf4 gene expression, however, was not affected by forced NICD expression (Fig. 1C), since it is suggested that the suppression of goblet cell phenotypic gene expression by Notch signaling is independent of Klf4 expression.

To assess how Notch signaling suppresses the gene expression of Hath1, we selected the Hes1 and HeyL genes as possible suppressors, based on previous identification of the Hes family genes induced by NICD in LS174T cells using a microarray system.[8] We confirmed that the gene expression of Hes1 and HeyL was markedly induced by NICD expression (Fig. 1D,E).

Hes1 But Not HeyL Suppresses *Hath1* Gene Expression in Human IECs, Resulting in the Decrease of MUC2 Gene Expression

To assess which genes suppress the *Hath1* gene expression, we generated cells (LS174T Tet-on Hes1 cells and LS174T Tet-on HeyL cells) in which either Hes1 or HeyL is induced by DOX using the Tet-on system, respectively. Forced expression of Hes1 alone showed a significant decrease of MUC2 gene expression following the decrease of *Hath1* gene expression (Fig. 2A,B). In contrast, HeyL induction alone did not change the expression of either MUC2 (Fig. 2A) or Hath1 genes (Fig. 2B). Moreover, neither Hes1 nor HeyL induction affected Klf4 gene expression (Fig. 2C). These results are compatible with previous reports that the depletion of Hes1 in a mouse model upregulated Atoh1 mRNA expression in intestinal epithelial cells, resulting in the hyperplasia of the goblet cells.[15] Conversely, the finding that Klf4 was not affected by the Notch signaling differs from previous reports.[16]

Hes1 Expression Alone Is a Sufficient Condition for the Repression of the Phenotypic Gene Expression of Goblet Cells by Notch Signaling

To further analyze the functional role of Notch signaling in the differentiation of IECs, we next asked whether Hes1 expression alone is enough to compensate for the suppression of *Hath1* gene expression in Notch signaling. To inhibit the Notch signaling, LS174T Tet-on Hes1 cells were treated with gamma-secretase inhibitor (GSI), which prevents the separation of NICD from the Notch receptor. Notch signal inhibition by GSI treatment alone showed a significant decrease of Hes1 gene expression (Fig. 3A), in contrast to marked induction of MUC2

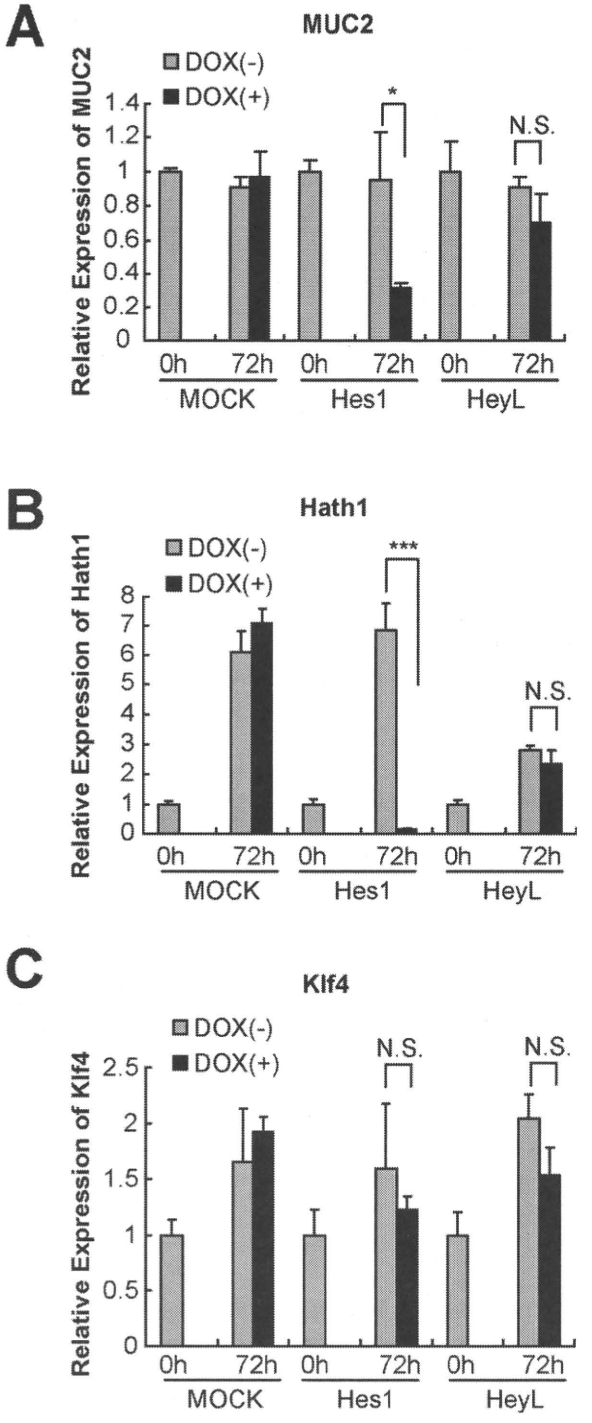

FIGURE 2. Gene alternation in LS174T cells by the expression of either Hes1 or HeyL. (A) Hes1 or HeyL was induced by DOX in LS174T Tet-on Hes1 cells or LS174T Tet-on HeyL cells, respectively. Hes1 induction significantly decreased MUC2 gene expression. (B) Hes1 induction resulted in a significant decrease of Hath1. (C) Neither Hes1 nor HeyL induction affected Klf4 gene expression. (*$P < 0.05$, ***$P < 0.001$, $n = 3$).

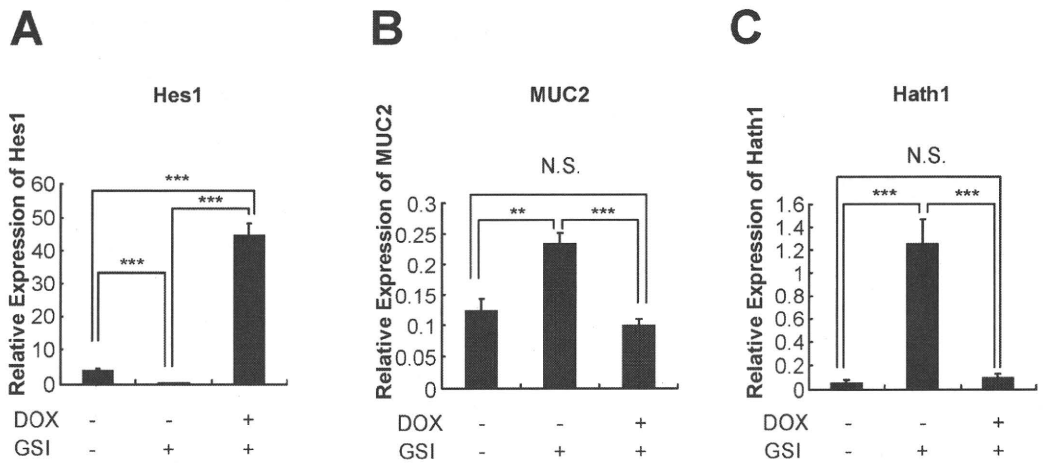

FIGURE 3. Hes1 expression is enough to suppress intestinal cell differentiation by Notch signaling. (A) LS174T Tet-on Hes1 cells were treated with GSI, which prevents the separation of NICD from the Notch receptor. GSI treatment alone significantly decreased Hes1 gene expression. Hes1 was induced by DOX in addition to GSI. (B) GSI markedly induced MUC2 gene expression. Hes1 induction by DOX in GSI-treated cells restored MUC2 gene expression to the level in untreated cells. (C) GSI markedly induced *Hath1* gene expression. Hes1 induction by DOX in GSI-treated cells restored *Hath1* gene expression to the level in untreated cells. (**$P < 0.01$, ***$P < 0.001$, $n = 3$).

gene expression (Fig. 3B) following the induction of the *Hath1* gene (Fig. 3C). Interestingly, the Hes1 gene was expressed by DOX when Notch signaling was inhibited by GSI (Fig. 3A), while Hath1 expression was restored to the level in untreated cells (Fig. 3C). Moreover, MUC2 gene expression was also decreased by Hes1 expression alone (Fig. 3B).

These results indicate that Hes1 might be a mainstream of Notch signaling to suppress the phenotypic gene expression of goblet cells in human intestine.

Previous results raised the question of whether Hath1 is essential for expression of the MUC2 gene by Notch signaling inhibition. To assess the importance of the *Hath1* gene for MUC2 expression, the effect of silencing the *Hath1* gene using siRNA system was examined in LS174T cells in the Notch signaling-inhibited state. *Hath1* gene silencing resulted in cancellation of the *Hath1* gene expression induced by GSI treatment and restoration of MUC2 expression to the level in untreated cells (Supporting Information Fig. 1).

These results together suggest that Notch signaling affects the gene expression of Hath1 but not Klf4 to decide the fate of IECs.

HES1 Suppresses the Transcriptional Activity of Hath1 Via the 5′ Promoter Region

It has been reported that expression of Math1, the mouse homolog of Atoh1, was suppressed by ZIC1 or HIC1 via its 3′ region.[12,17] However, it has never been shown how Hes1 suppresses the transcriptional activity of Hath1 via Notch signaling. To assess the regulation of Hath1 transcriptional activity, we constructed a reporter plasmid containing the 1000-bp upstream 5′ region of Hath1. Hath1 reporter plasmid was transfected into LS174T Tet-on Hes1 cells or LS174T cells transfected with a mock plasmid. Hes1 induction by DOX showed a significant decrease of the transcriptional activity on Hath1, whereas the mock plasmid did not change its transcriptional activity (Fig. 4A). We then found three regions that matched the consensus sequence for binding Hes1, the Class C site,[18] in the 1000-bp upstream region of Hath1. We therefore constructed a reporter plasmid in which all regions of the Hes1 binding site in the 1000-bp upstream region of Hath1 were deleted. As expected, reporter activity of the deletion mutant construct was not suppressed by Hes1 expression. We next constructed mutants in which one of the binding sites of Hes1 in the 1000-bp upstream region of Hath1 was deleted. Interestingly, only the mutant construct lacking the second region of the Hes1 binding site was not affected by Hes1, indicating that Hes1 might directly suppress the Hath1 transcriptional activity to bind to the second region of the Hes1 binding site (Fig. 4A).

In chicken and mouse models, Atoh1 expression is regulated only by the 3′ region of Atoh1 that contains both the enhancer region and the repressor region.[12,19] We also found a homologous sequence of the enhancer region in the 3′ region of Hath1, and a Hes1 binding site in this enhancer region of Hath1. We therefore constructed a Hath1 reporter plasmid containing the 3′ region of Hath1 behind the luciferase sequence. As before, Hes1 suppressed Hath1 transcriptional activity. Moreover, deletion mutants of the Hes1 binding site in the 5′ region of Hath1 were also unaffected by Hes1 expression, indicating that the Hes1 binding site of the 3′ region might not affect Hath1 suppression by Hes1 (Fig. 4B).

HES1 Binds Directly to the 5′ Promoter Region of Hath1

To confirm the binding of Hes1 to Hath1 promoter region, we performed a ChIP assay. The region immunoprecipitated by Hes1 antibody was amplified only in the 5′ region

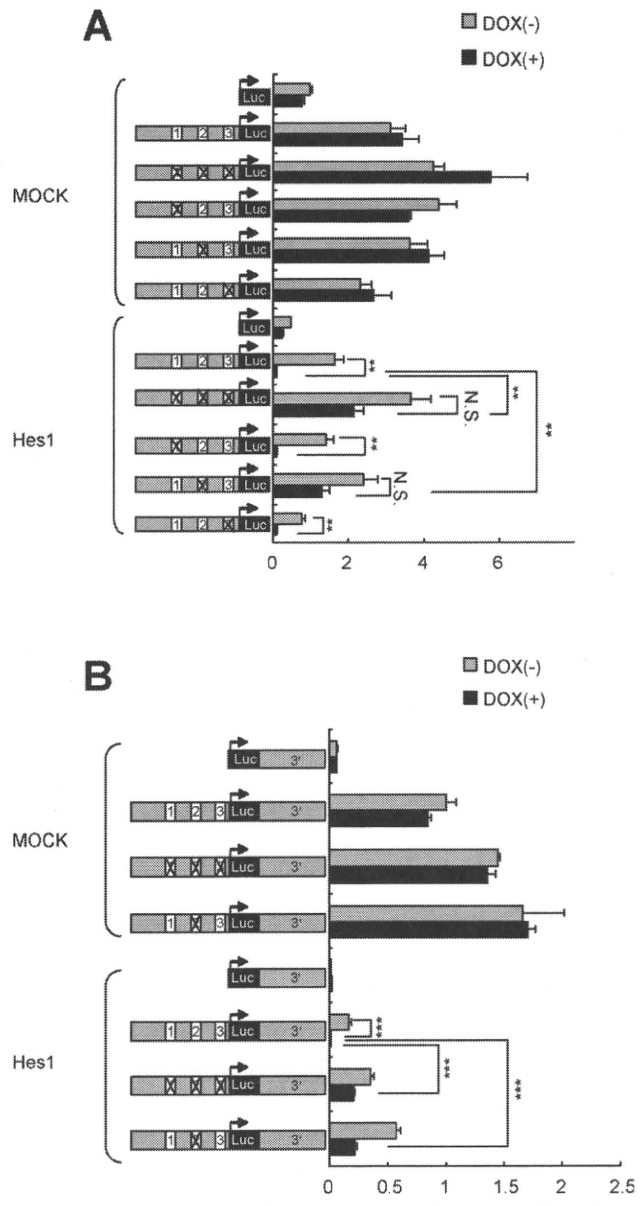

FIGURE 4. Hes1 regulates the transcriptional activity of Hath1 via 5′ promoter region. (A) 5′ Hath1 reporter plasmid containing the 1000-bp upstream region of Hath1 was transfected into LS174T Tet-on Hes1 cells and LS174T cells transfected with a mock plasmid. The induction of Hes1 by DOX significantly decreased the transcriptional activity on Hath1, whereas the transcriptional activity of the mock plasmid did not change. Three regions that matched the consensus sequence for binding Hes1, the Class C site, in the 1000-bp upstream region of Hath1 are indicated as square numbers. Reporter activity of a mutant with all regions of the Hes1 binding site deleted was not suppressed by Hes1 expression. A mutant construct in which only the second region of the Hes1 binding site was deleted was also unaffected by Hes1. (B) Hath1 reporter plasmid containing the 3′ enhancer region of Hath1 behind the luciferase sequence was inserted into 5′ Hath1 reporter plasmid. Hes1 also suppressed Hath1 transcriptional activity enhanced by 3′ enhancer region. The deletion mutants of the Hes1 binding site in the 5′ region of Hath1 were also unaffected by Hes1 expression (B). (**$P < 0.01$, ***$P < 0.001$, $n = 3$).

including the Hes1 binding sites but not 3′ region of the Hes1 binding sites (Fig. 5B), supporting the idea that Hes1 binds directly to the 5′region of Hath1 to suppress the transcriptional activity in IEC.

Hes1 Does Not Completely Block the Transcriptional Activity of Hath1 Promoted by CDX2

To clarify the balance between the enhancer and the repressor in Hath1 transcriptional activity, we next assessed whether CDX2, which promotes *Atoh1* gene transcription in mice, is affected by Notch signaling on Hath1 transcription. Treatment with GSI showed slight induction of CDX2 in LS174T cells (Fig. 6A). Moreover, HES1 expression did not affect the expression of CDX2 (Fig. 6B), suggesting that the expression of CDX2 may be independent of Notch signaling. To assess the effect of CDX2 on Hath1 transcription regulated by HES1, a reporter assay of Hath1 was performed. Although CDX2 did not promote Hath1 transcription via the 5′ promoter region of Hath1 (Fig. 6C), CDX2 cotransfected with the reporter plasmid containing the 3′ enhancer region of Hath1 showed significant increase of transcriptional activity of Hath1 (Fig. 6D). Interestingly, the transcriptional activity of Hath1 promoted by CDX2 was not suppressed by Hes1 induction in LS174T tet-HES1 cells. These results suggest that Hes1 at the 5′ region of Hath1 could not completely abrogate the transcriptional activity of Hath1 promoted via the 3′ enhancer region by CDX2, and *Hath1* gene expression might be regulated by the balance between HES1 and CDX2.

Hath1 Protein Expression Is Decreased in the Goblet Cell Depletion of UC

We finally assessed whether Hath1 is decreased in colon mucosa with goblet cell depletion in line with the former results in vitro. In normal colonic mucosa, Hath1 and CDX2 were expressed in almost all IECs. In contrast, Hes1 was expressed in IECs situated in the lower half of the villi (Fig. 7). In UC patients, both Hath1 and CDX2 disappeared, while Hes1-positive cells were extended at the top of the villi (Fig. 7), indicating that the suppression of Hath1 in goblet cell depletion might be caused by both the disappearance of CDX2 and the extension of Hes1-positive cells.

DISCUSSION

This study reveals for the first time that Hes1 directly suppresses *Hath1* gene expression via the Notch signal, indicating that downregulation of Hath1 is associated with goblet cell depletion in human UC in combination with the disappearance of CDX2. Previous reports have suggested that Notch signaling suppressed the phenotypic gene expression of goblet cells by suppressing *Atoh1* gene expression,[5] although it remains unknown how Notch signaling suppresses

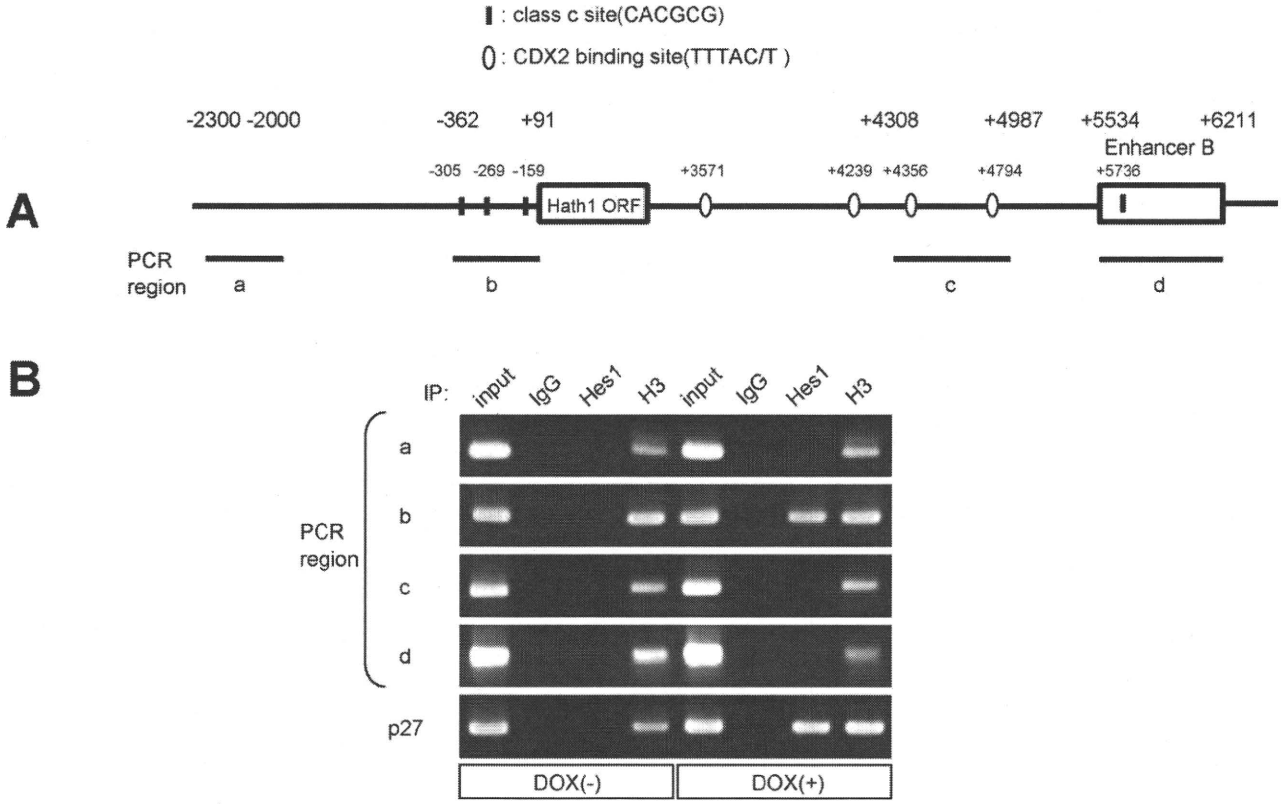

FIGURE 5. Hes1 binds to 5′ Hath1 promoter region. (A) Schematic presentation of Hath1 genome. (B) ChIP assay was performed using LS174T Tet-on Hes1 cells with or without DOX treatment for 24 hours. Each region indicated by a letter in (A) was amplified from the immunoprecipitant by each antibody. The amplification of p27 from the immunoprecipitant by Hes1 antibody was confirmed to be the known region of the Hes1 binding site. Only the 5′ region including the Hes1 binding sites of Hath1 (region b) was amplified from the immunoprecipitant by Hes1 antibody under the induction of Hes1 expression by DOX.

Hathl gene expression. We first found that Hes1, but not HeyL, was necessary and sufficient for the suppression of *Hathl* gene expression by Notch signaling in IEC. Canonical Notch signaling leads to transcriptional activation of Hes family and Hey family genes such as Hes1, Hes5, Hes7, Hey1, Hey2, and HeyL by binding NICD to RBP-Jk.[20] Hes and Hey family genes play important roles in the differentiation of various tissues,[21,22] but it has not been clarified how the function of each gene is assigned via Notch signaling. While we found that all Hes and Hey family genes were upregulated by NICD expression in intestinal cells, we also noticed that Hes1 and HeyL were exorbitantly expressed by NICD than other Hes and Hey family genes (data not shown), suggesting that the functional assignment of Notch signaling is regulated by the quantity of each Hes and Hey family gene expressed. HeyL has been identified as one of the target genes of Notch3 receptor, because HeyL is expressed in smooth muscle cells of the digestive tract and the vasculature following Notch3 expression in later stages of development.[23] In this study, we could not identify the function of HeyL in goblet cell differentiation; rather, its function is expected to be assessed in future study of the effect of Notch signaling on IEC.

On the other hand, we found that Hes1 is critical for the differentiation into goblet cells via Notch signaling, since the binding of HES1 to the Hath1 5′ promoter region silences *Hathl* gene expression. Although the 3′ region of Atoh1 has been characterized as the enhancer and repressor region to regulate *Hathl* gene expression by CDX2, Zic1, and Hic1, the function of the 5′ region of Atoh1 has not been clarified. This study revealed that the 5′ region of Hath1 is necessary not only for basic transcription but also for the regulation by HES1 via Notch signaling to presumably suppress the transcriptional activity of the basic transcription factors. It has been reported that Hes1 binds not only to the N-box sequence but also to class C sites to suppress the expression of genes such as $P27^{kip1}$[18] and achaete-scute homolog-1,[24] through which it plays a central role in cell proliferation and differentiation, respectively. In this study we identified a class C site at position −289 of the 5′ region of Hath1, playing a crucial role in the regulation of *Hathl* gene expression by the Notch signal. We therefore suspected that Hes1 might completely shut out the transcriptional activity via the

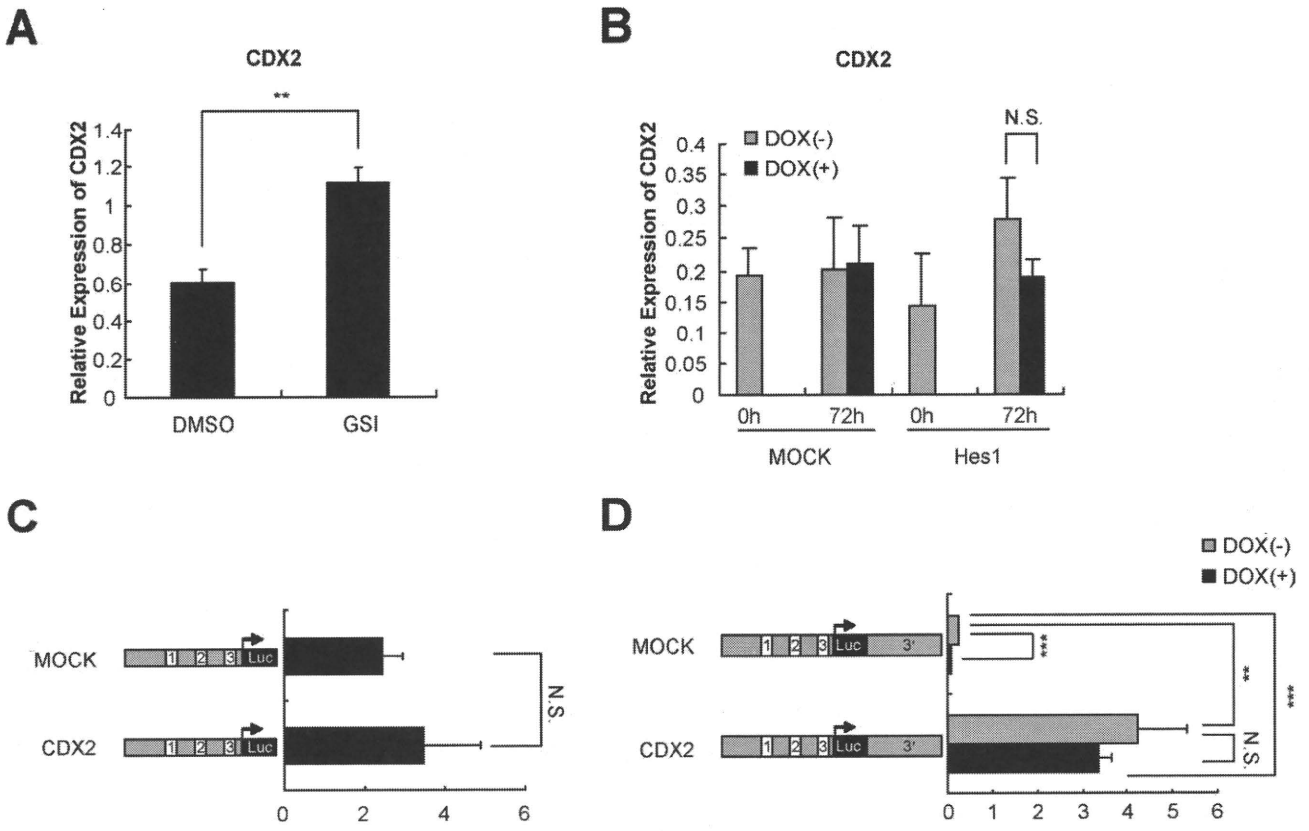

FIGURE 6. CDX2 enhances the transcriptional activity of Hath1 independently of Notch signaling. (A) *CDX2* gene expression was analyzed by treatment of LS174T cells with GSI for 72 hours. CDX2 was slightly upregulated by Notch signal inhibition. (B) *CDX2* gene expression was analyzed by the Hes1 expression induced by DOX in LS174T Tet-on Hes1 cells. *CDX2* gene expression was not affected by Hes1 expression. (C) Transcriptional activity of Hath1 via the 5′ region by CDX2 was assessed in LS174T cells for 72 hours after transfection of both the *CDX2* gene and 5′ Hath1 reporter plasmid. CDX2 did not affect the transcriptional activity via the 5′ promoter region of Hath1. (D) HES1 did not suppress the transcriptional activity via the 3′ region of Hath1 by forced expression of CDX2. The transcriptional activity of Hath1 was assessed for 72 hours after transfection of both the *CDX2* gene and 3′ Hath1 reporter plasmid with or without DOX in LS174T Tet-on HES1 cells. (**$P < 0.01$, ***$P < 0.001$, $n = 3$).

3′ enhancer region, but that forced expression of CDX2 could induce the transcriptional activity of Hath1 even with Hes1 expression. Moreover, the expression of CDX2 was not affected by Notch signaling, suggesting that CDX2 and HES1 independently regulate *Hath1* gene expression. Thus, regulation by Hes1 via Notch signaling is not sufficient to suppress the gene transcription of *Hath1*, indicating that the transcriptional activity of Hath1 is regulated by the balance between CDX2 and HES1 expression.

Importantly, the present study also indicated that Hath1 is essential to regulate goblet cell formation in UC. Although the expression of Hath1 in inflamed mucosa of UC has been reported,[25] the correlation between goblet cell content and Hath1 expression in UC has not been elucidated. We confirmed that Hath1 was expressed in inflamed mucosa with conserved goblet cell formation in UC (data not shown), since goblet cell content might correlate with Hath1 expression in UC. In Atoh1-deficient mice, secretory lineages of IEC including goblet cells are completely lost,[9,26] indicating that Hath1 might have the function of not only mucus production but also differentiation toward goblet cells in human intestine.

Moreover, this study suggested that goblet cell depletion in UC caused by the disappearance of Hath1 required not only HES1 expression but also CDX2 suppression of IEC. CDX2 has been reported to be downregulated in UC mucosa,[27] but it remains unknown how CDX2 expression is suppressed by colonic inflammation even though CDX2 is upregulated by inflammation in the esophagus and stomach.[28,29] One previous report indicated that CDX2 expression is suppressed by hypoxia inducible factor 1 (HIF1).[30] Another report found that HIF1 is overexpressed in UC mucosa,[31] suggesting that HIF1 might suppress CDX2 expression in UC. Whatever the case, the regulation of CDX2 expression of IEC should be assessed to clarify the mechanism of goblet cell depletion in UC.

In conclusion, we have revealed for the first time that Hes1 is sufficient to suppress *Hath1* gene transcription via the Notch signal, but insufficient to suppress *Hath1* gene transcription by CDX2. The cooperation between Hes1 and

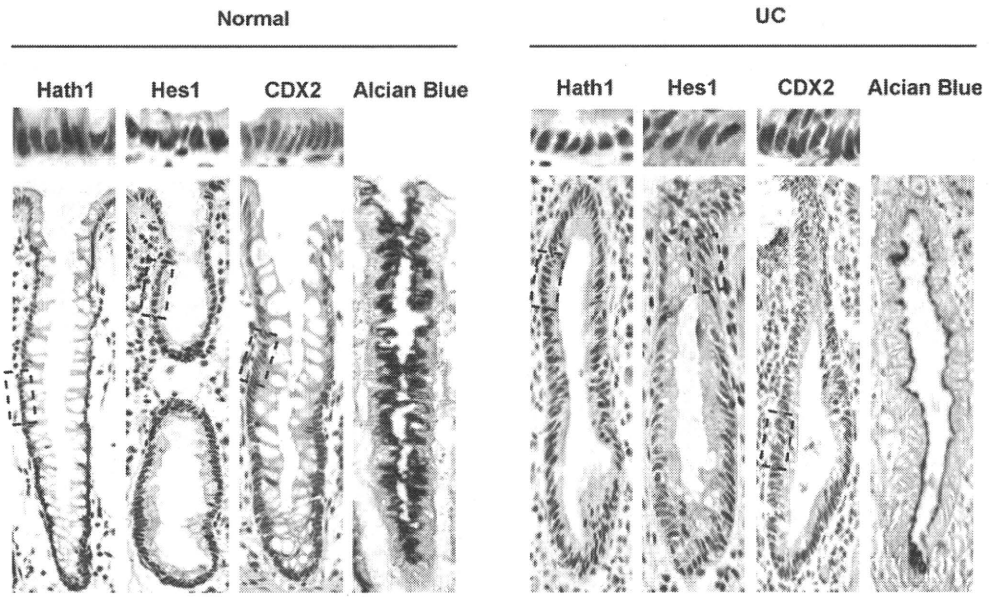

FIGURE 7. Immunohistochemistry of intestinal mucosa in UC. In normal colonic mucosa, Hath1 and CDX2 were expressed in most IEC. Hes1 was expressed in intestinal epithelial cells in the lower half of villi. In UC mucosa with goblet cell depletion, neither Hath1 nor CDX2 was expressed, whereas Hes1 was expressed up to the top of the villi. Upper column shows magnified view of the upper villus areas identified by dashed line in the lower column. Blue staining with Alcian blue represents goblet cells. The examination was performed by using the sections from three different individuals.

CDX2 is important to regulate *Hath1* gene expression, which is involved in goblet cell formation in UC. More detailed analysis of Hath1 expression at various stages of UC or other enteritis diseases associated with goblet cell depletion will lead us understand the regulation of Hath1 reduction under the inflammation state with various cytokines and inflammatory cells infiltration. Finally, elucidation of the mechanism of goblet cell depletion in UC will help us to develop novel therapies for strengthening the barrier function of colonic mucosa.

REFERENCES

1. Booth C, Brady G, Potten CS. Crowd control in the crypt. *Nat Med.* 2002;8:1360–1361.
2. El-Assal ON, Besner GE. HB-EGF enhances restitution after intestinal ischemia/reperfusion via PI3K/Akt and MEK/ERK1/2 activation. *Gastroenterology.* 2005;129:609–625.
3. Haramis AP, Begthel H, van den Born M, et al. De novo crypt formation and juvenile polyposis on BMP inhibition in mouse intestine. *Science.* 2004;303:1684–1686.
4. Clevers H. Wnt/beta-catenin signaling in development and disease. *Cell.* 2006;127:469–480.
5. Fre S, Huyghe M, Mourikis P, et al. Notch signals control the fate of immature progenitor cells in the intestine. *Nature.* 2005;435:964–968.
6. Oshima S, Nakamura T, Namiki S, et al. Interferon regulatory factor 1 (IRF-1) and IRF-2 distinctively up-regulate gene expression and production of interleukin-7 in human intestinal epithelial cells. *Mol Cell Biol.* 2004;24:6298–6310.
7. Crosnier C, Stamataki D, Lewis J. Organizing cell renewal in the intestine: stem cells, signals and combinatorial control. *Nat Rev Genet.* 2006;7:349–359.
8. Okamoto R, Tsuchiya K, Nemoto Y, et al. Requirement of Notch activation during regeneration of the intestinal epithelia. *Am J Physiol Gastrointest Liver Physiol.* 2009;296:G23–35.
9. Yang Q, Bermingham N, Finegold M, et al. Requirement of Math1 for secretory cell lineage commitment in the mouse intestine. *Science.* 2001;294:2155–2158.
10. Tsuchiya K, Nakamura T, Okamoto R, et al. Reciprocal targeting of Hath1 and beta-catenin by Wnt glycogen synthase kinase 3beta in human colon cancer. *Gastroenterology.* 2007;132:208–220.
11. Helms A, Abney A, Ben-Arie N, et al. Autoregulation and multiple enhancers control Math1 expression in the developing nervous system. *Development.* 2000;127:1185–1196.
12. Ebert PJ, Timmer JR, Nakada Y, et al. Zic1 represses Math1 expression via interactions with the Math1 enhancer and modulation of Math1 autoregulation. *Development.* 2003;130:1949–1959.
13. Murata K, Hattori M, Hirai N, et al. Hes1 directly controls cell proliferation through the transcriptional repression of p27Kip1. *Mol Cell Biol.* 2005;25:4262–4271.
14. Katz JP, Perreault N, Goldstein BG, et al. The zinc-finger transcription factor Klf4 is required for terminal differentiation of goblet cells in the colon. *Development.* 2002;129:2619–2628.
15. Jensen J, Pedersen EE, Galante P, et al. Control of endodermal endocrine development by Hes-1. *Nat Genet.* 2000;24:36–44.
16. Zheng H, Pritchard D, Yang X, et al. KLF4 gene expression is inhibited by the notch signaling pathway that controls goblet cell differentiation in mouse gastrointestinal tract. *Am J Physiol Gastrointest Liver Physiol.* 2009;296:G490–498.
17. Briggs KJ, Corcoran-Schwartz IM, Zhang W, et al. Cooperation between the Hic1 and Ptch1 tumor suppressors in medulloblastoma. *Genes Dev.* 2008;22:770–785.
18. Murata K, Hattori M, Hirai N, et al. Hes1 directly controls cell proliferation through the transcriptional repression of p27Kip1. *Mol Cell Biol.* 2005;25:4262–4271.
19. Mutoh H, Sakamoto H, Hayakawa H, et al. The intestine-specific homeobox gene Cdx2 induces expression of the basic helix-loop-helix transcription factor Math1. *Differentiation.* 2006;74:313–321.
20. Katoh M. Notch signaling in gastrointestinal tract (review). *Int J Oncol.* 2007;30:247–251.
21. Kageyama R, Ohtsuka T, Kobayashi T. The Hes gene family: repressors and oscillators that orchestrate embryogenesis. *Development.* 2007; 134:1243–1251.